Acta Crystallographica Section F
Structural Biology and Crystallization Communications
ISSN 1744-3091

Crystallization and preliminary X-ray analysis of pyridoxine 4-oxidase, the first enzyme in pyridoxine degradation pathway I

Andrew Njagi Mugo,[a] Jun Kobayashi,[b] Bunzo Mikami,[b] Kouhei Ohnishi[c] and Toshiharu Yagi[a]*

[a]Faculty of Agriculture and Agricultural Science Program, Graduate School of Integral Arts and Science, Kochi University, Nankoku, Kochi 783-8502, Japan, [b]Division of Applied Life Sciences, Graduate School of Agriculture, Kyoto University, Gokasho, Uji, Kyoto 611-0011, Japan, and [c]Research Institute of Molecular Genetics, Kochi University, Nankoku, Kochi 783-8502, Japan

Correspondence e-mail: yagito@kochi-u.ac.jp

Received 13 October 2011
Accepted 16 November 2011

Vitamin B_6-degradation pathway I has recently been identified in *Mesorhizobium loti* MAFF303099. Pyridoxine 4-oxidase, an FAD-dependent enzyme, is the first enzyme in this pathway and catalyzes the irreversible oxidation of pyridoxine to pyridoxal. The enzyme was overexpressed in *Escherichia coli* with a His_6 tag and purified. The recombinant enzyme was crystallized at 277 K by the sitting-drop vapour-diffusion method using PEG 4000 as the precipitant. The crystal, which belonged to space group $P2_12_12_1$ with unit-cell parameters a = 62.38, b = 79.44, c = 136.43 Å, diffracted to 2.2 Å resolution. The calculated V_M value (3.19 Å^3 Da^{-1}) suggested that the asymmetric unit contained one molecule.

1. Introduction

Pyridoxine 4-oxidase (EC 1.1.3.12) participates in the degradation of vitamin B_6. It contains FAD and catalyzes the oxidation of pyridoxine to pyridoxal (Fig. 1). Two pathways for degradation of the free forms of vitamin B_6 (pyridoxine, pyridoxal and pyridoxamine) have been identified in soil microbes that can use vitamin B_6 as a sole source of carbon and nitrogen. Pathway I has been found in *Pseudomonas* sp. MA-1 (Burg *et al.*, 1960) and *Mesorhizobium loti* (Yuan *et al.*, 2004) and pathway II in *Pseudomonas* sp. 1A and *Arthrobacter* sp. Cr-7 (Nelson & Snell, 1986). In pathway I, pyridoxine is first oxidized to pyridoxal by pyridoxine 4-oxidase and the pyridoxal is then degraded to succinic semialdehyde, acetic acid, carbon dioxide and ammonia through seven enzymatic steps. In pathway II, pyridoxine is first oxidized to 5-pyridoxal by pyridoxine 5-oxidase and the 5-pyridoxal is then degraded to 2-hydroxymethyl succinic semialdehyde, acetic acid, ammonia and carbon dioxide through five enzymatic steps.

Pyridoxine 4-oxidase has been purified from three bacteria: *Pseudomonas* sp. MA-1 (Sundaram & Snell, 1969), *Microbacterium luteolum* (Kaneda *et al.*, 2002) and *M. loti* (Yuan *et al.*, 2004). The enzymes from *M. loti* and *M. luteolum* are monomeric and have molecular weights of 55 000 and 54 000, respectively. Pyridoxine 4-oxidase shows high hydrogen-donor specificity: only three pyridinium compounds, for example pyridine 4-methanol, were used as substrates, with very low reactivity (less than 0.15% of the reactivity toward pyridoxine). The enzyme showed no reactivity toward pyridoxine 5′-phosphate, which is a precursor of pyridoxal 5′-phosphate, a coenzyme form of vitamin B_6. The amino-acid sequences of the pyridoxine 4-oxidases from *M. loti* and *M. luteolum* showed high identity (66%). The sequences showed that the pyridoxine 4-oxidases belong to the glucose–methanol–choline (GMC) oxidoreductase family as they contain two GMC oxidoreductase signature sequences (Prosite).

GMC oxidoreductase C family enzymes are well known FAD-dependent oxidoreductases and there are 4172 members in the Pfam

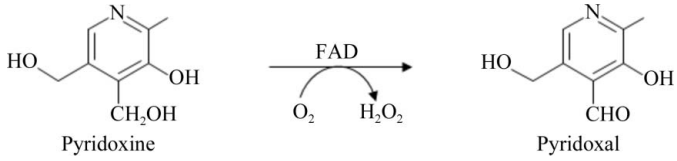

Figure 1
The reaction catalyzed by pyridoxine 4-oxidase.

database (as of October 2010). GMC oxidoreductase family enzymes show diverse catalytic activities towards compounds with a CH—OH group (Cavener, 1992). Enzymes in this family have a conserved ADP-binding sequence ($\beta\alpha\beta$-fold) near their N-termini, which is involved in FAD binding (Dym & Eisenberg, 2001), and one or two signature sequences corresponding to residues 94–117 and 268–282, respectively, in *M. loti* pyridoxine 4-oxidase. In contrast to the N-terminal region (residues 19–44), the function of the C-terminal region (residues 460–520) of the enzymes is not known. Interestingly, pyridoxine 4-oxidase has the signature 2 sequence of the regulator of chromosome condensation (RCC1) protein at residues 500–510. Because the gene encoding pyridoxine 4-oxidase is located next to a gene encoding a repressor protein (PyrR), which may control the expression of the cluster of enzymes involved in the degradation pathway, the function of residues 500–510 should be elucidated.

In order to elucidate the catalytic mechanism and the function of residues 500–510 of pyridoxine 4-oxidase, determination of the three-dimensional structure of the enzyme is necessary. Here, we report the crystallization and preliminary X-ray diffraction studies of pyridoxine 4-oxidase from *M. loti*.

2. Materials and methods

2.1. Overexpression and purification of pyridoxine 4-oxidase

Although the recombinant enzyme has been purified (Yuan *et al.*, 2004), it could not be crystallized for unknown reasons. Here, pyridoxine 4-oxidase (PNox) with a His_6 tag was prepared and used for crystallization. A *mll6785* gene fragment was prepared from pET-mll6785 constructed previously (Yuan *et al.*, 2004) by digestion with *Xba*I and *Sal*I, and was inserted into pTrc99A (Amersham Biosciences) to yield pTrc99A-mll6785. The His_6-tag-encoding nucleotide was inserted into the 3′-terminus of pTrc99A-mll6785 by inverse PCR with a KOD$^+$ Mutagenesis Kit (TOYOBO) to yield pTrc99A-mll6785-his according to the instruction manual. The primers used were 5′-CACCACCACCACCACCACTAAGTCGACCTGCAGGCATGCAAGCTT-3′ (pTrc99A-mll6785-his-F) and 5′-GTACTGTCGGGCGAAAGTCTCG-3′ (pTrc99A-mll6785-his-R). *Escherichia coli* JM109 cells were co-transformed with pTrc99A-mll6785-his and pKY206 carrying chaperonin genes (Mizobata *et al.*, 1992). The transformed cells were grown in 5 ml LB medium containing ampicillin (50 µg ml^{-1}), tetracycline (12.5 µg ml^{-1}) and riboflavin (50 µg ml^{-1}) at 295 K for 24 h. The broth was then transferred to 200 ml of the same medium and the inoculated cells were grown at 296 K for 48 h. The cells were harvested by centrifugation at 8000 rev min^{-1} for 10 min at 277 K and washed with 0.9%(*w*/*v*) NaCl. The harvested cells (2 g wet weight) were suspended in 20 ml buffer *A* [20 m*M* potassium phosphate buffer pH 8.0, 10%(*w*/*v*) glycerol, 5 µ*M* FAD, 10 m*M* β-mercaptoethanol, 0.01%(*v*/*v*) Tween 20] containing 300 m*M* NaCl and 10 m*M* imidazole. The suspension was sonicated on ice for 4 min with a model W-220 sonicator (Heat Systems-Ultrasonics, Farmingdale, New York, USA). A cell extract was obtained by centrifugation at 10 000*g* for 10 min at 277 K; the precipitate was resuspended again in buffer *A*, sonicated and centrifuged. The combined supernatants were used as the crude extract. The crude extract was applied onto an Ni–NTA agarose column (1.6 × 10 cm, Qiagen) equilibrated with buffer *A* containing 300 m*M* NaCl and 20 m*M* imidazole. The column was washed until the A_{280} of the eluted solution decreased to below 0.01 and the enzyme was then eluted with buffer *A* containing 300 m*M* NaCl and 100 m*M* imidazole. The eluted enzyme solution was thoroughly dialyzed against buffer *A* and then applied onto a QA52 column (1.6 × 2.5 cm, Whatman) equilibrated with buffer *A*. The enzyme was eluted with buffer *A* containing 0.2 *M* NaCl. The eluted enzyme solution was thoroughly dialyzed at 277 K against the crystallization buffer [50 m*M* Tris–HCl pH 8.0, 10%(*w*/*v*) glycerol, 5 µ*M* FAD, 0.1%(*v*/*v*) β-mercaptoethanol, 0.01%(*v*/*v*) Tween 20].

2.2. Enzyme assay

PNox activity was determined as described previously (Yuan *et al.*, 2004). Briefly, a reaction mixture (1 ml) consisting of 0.1 *M* Tris–HCl pH 8.0, 5 m*M* pyridoxine, 5 µ*M* FAD and the enzyme was incubated aerobically for 10 min at 303 K. The yellow colour produced by the Schiff base formed by the reaction between pyridoxal and Tris base was measured by the absorbance at 415 nm. One unit of enzyme was defined as the amount that catalysed the formation of 1 µmol pyridoxal per minute. Protein concentrations were measured by the protein-dye method (Bradford, 1976).

2.3. Crystallization and X-ray analysis

The purified enzyme was concentrated to 10 mg ml^{-1} using an Amicon Ultra-4 filter (Millipore, Billerica, USA). Crystallization conditions were screened using the Crystallization Basic Kit for Proteins (Sigma–Aldrich Chemie, Steinheim, Germany) and Wizard I and II (Emerald BioSystems, Washington, USA) by the sitting-drop vapour-diffusion method. A mixture consisting of 2 µl enzyme solution and 2 µl reservoir solution was equilibrated against 100 µl reservoir solution at 277 K using CrystalClear Strips from Hampton Research (Laguna Niguel, California, USA). A low-quality crystal grew after one month with reservoir solution No. 41 [0.1 *M* HEPES–NaOH pH 7.5, 10%(*v*/*v*) 2-propanol, 20%(*w*/*v*) PEG 4000] from the Crystallization Basic Kit for Proteins. The crystal was crushed and suspended in 500 µl of a solution consisting of equal volumes of the crystallization buffer and reservoir solution No. 41 to yield a seeding solution. A mixture of 2 µl enzyme solution and reservoir solution No. 41 was equilibrated for 1 d against 100 µl reservoir solution at 277 K using CrystalClear Strips from Hampton Research. 0.1 µl of the crystal suspension was then added to the mixture. The micro-seeded solution was equilibrated against the reservoir solution at 277 K. Crystals grew within one month.

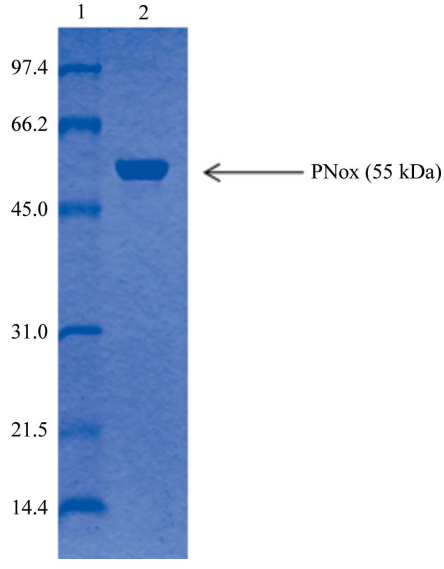

Figure 2
SDS–PAGE analysis of the purified pyridoxine 4-oxidase. Lane 1, molecular-weight markers (labelled in kDa). Lane 2, purified enzyme used for crystallization (4 µg).

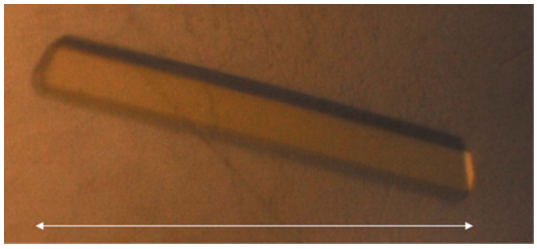

Figure 3
Crystal of pyridoxine 4-oxidase. The scale bar is 0.2 mm in length.

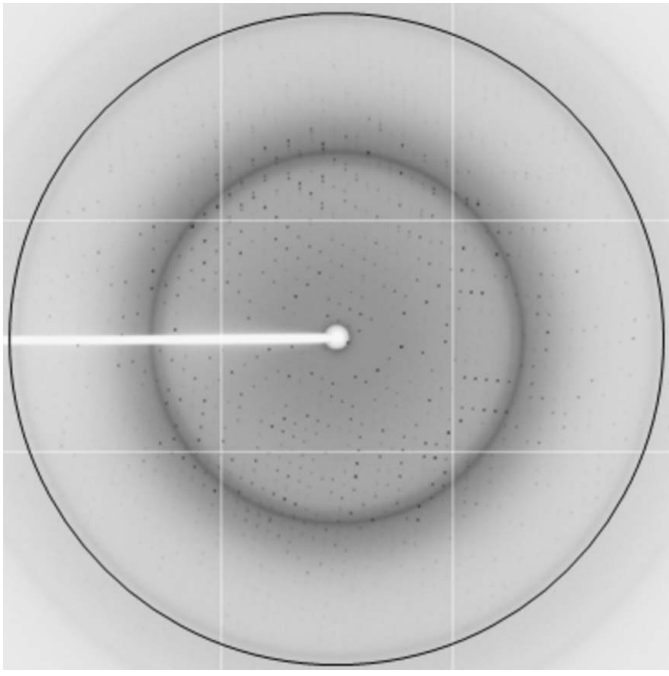

Figure 4
Diffraction image of pyridoxine 4-oxidase. The ring indicates a resolution of 2.2 Å.

A PNox crystal was picked out from a droplet and placed into a nitrogen-gas stream at 100 K without cryoprotectant treatment. X-ray diffraction images were obtained using an in-house Bruker Hi-Star multi-wire area detector coupled to a MAC Science M18XHF rotating-anode generator at Kyoto University. The final diffraction data for the selected crystal were collected at 100 K in a nitrogen-gas stream using an ADSC Quantum 315 CCD detector and synchrotron radiation of wavelength 1.00 Å at the BL38B1 station of SPring-8 (Hyogo, Japan). The crystal-to-detector distance was set to 300.0 mm. Oscillation images of 1.0° were recorded with an exposure time of 20 s.

3. Results and discussion

His_6-tagged pyridoxine 4-oxidase was successfully overexpressed in *E. coli* and purified, with significant enzyme activity being maintained. The results of SDS–PAGE analysis of the purified enzyme are shown in Fig. 2.

Crystals suitable for X-ray data collection were obtained (Fig. 3). The crystals yielded good diffraction images, as shown in Fig. 4. Diffraction data were obtained from the crystal in the resolution range 50.00–2.20 Å and were processed using the *HKL*-2000 program package (*DENZO* and *SCALEPACK*; Otwinowski & Minor, 1997). The crystal parameters and diffraction data statistics are summarized in Table 1. The data set was 99.8% complete at the resolution limit of 2.2 Å. The V_M value (the crystal volume per unit protein molecular weight; Matthews, 1968) was calculated to be 3.19 $Å^3$ Da^{-1} assuming the presence of one molecule of the enzyme in an asymmetric unit, with the solvent content being 61.42%. The V_M value and solvent content lie within the ranges usually found for protein crystals. The molecular-replacement method was performed using the *MOLREP* program from the *CCP*4 program suite (Winn *et al.*, 2011) with the structures of the glucose oxidases from *Aspergillus niger* and *Penicillium amagasakiense* (PDB entries 1cf3 and 1gpe; Wohlfahrt *et al.*, 1999) and of cholesterol oxidase (PDB entry 3gyi; Lyubimov *et al.*, 2009) as models, but a plausible solution could not be obtained.

We are currently using other available GMC oxidoreductase structures as search models for molecular replacement and independently preparing heavy-atom derivatives of the enzyme.

Table 1
Data-collection statistics for a crystal of PNox.

Values in parentheses are for the highest resolution shell.

X-ray source	BL38B1, SPring-8
Wavelength (Å)	1.000
Detector	ADSC Q315 CCD
Crystal system	Orthorhombic
Space group	$P2_12_12_1$
Unit-cell parameters (Å)	a = 62.380, b = 79.438, c = 136.429
Processing software	*HKL*-2000
Resolution limits (Å)	50.0–2.20 (2.24–2.20)
Measured reflections	303407 (14716)
Unique reflections	35380 (1752)
Completeness (%)	99.8 (99.5)
Multiplicity	8.6 (8.4)
$\langle I/\sigma(I)\rangle$	15.9 (6.4)
R_{merge} (%)†	7.3 (48.1)

† $R_{merge} = \sum_{hkl}\sum_i |I_i(hkl) - \langle I(hkl)\rangle| / \sum_{hkl}\sum_i I_i(hkl)$, where $I_i(hkl)$ is the intensity of observed reflection hkl and $\langle I(hkl)\rangle$ is the average intensity for multiple measurements.

We thank Drs K. Hasegawa and S. Baba of the Japan Synchrotron Radiation Research Institute (JASRI) for their kind help in the data collection. X-ray data collection at BL38B1 of SPring-8 was carried out with the approval of the organizing committee of SPring-8.

References

Bradford, M. M. (1976). *Anal. Chem.* **72**, 248–254.
Burg, R. W., Rodwell, V. W. & Snell, E. E. (1960). *J. Biol. Chem.* **235**, 1164–1169.
Cavener, D. R. (1992). *J. Mol. Biol.* **223**, 811–814.
Dym, O. & Eisenberg, D. (2001). *Protein Sci.* **10**, 1712–1728.
Kaneda, Y., Ohnishi, K. & Yagi, T. (2002). *Biochemistry*, **66**, 1022–1031.
Lyubimov, A. Y., Chen, L., Sampson, N. S. & Vrielink, A. (2009). *Acta Cryst.* D**65**, 1222–1231.
Matthews, B. W. (1968). *J. Mol. Biol.* **33**, 491–497.
Mizobata, T., Akiyama, Y., Ito, K., Yumoto, N. & Kawata, Y. (1992). *J. Biol. Chem.* **267**, 17773–17779.
Nelson, M. J. & Snell, E. E. (1986). *J. Biol. Chem.* **261**, 15115–15120.
Otwinowski, Z. & Minor, W. (1997). *Methods Enzymol.* **276**, 307–326.
Sundaram, T. K. & Snell, E. E. (1969). *J. Biol. Chem.* **244**, 2577–2584.
Winn, M. D. *et al.* (2011). *Acta Cryst.* D**67**, 235–242.
Wohlfahrt, G., Witt, S., Hendle, J., Schomburg, D., Kalisz, H. M. & Hecht, H.-J. (1999). *Acta Cryst.* D**55**, 969–977.
Yuan, B., Yoshikane, Y., Yokochi, N., Ohnishi, K. & Yagi, T. (2004). *FEMS Microbiol. Lett.* **234**, 225–230.